Mon. Not. R. astr. Soc. (1980) **192,** 505–519

Roberts 22: a bipolar nebula with OH emission

D. A. Allen *Anglo-Australian Observatory, PO Box 296, Epping NSW 2121, Australia*

A. R. Hyland *Mount Stromlo and Siding Spring Observatory, Private Bag, Woden, ACT 2606, Australia, and Institute of Astronomy, Madingley Road, Cambridge CB3 0HA*

J. L. Caswell *Division of Radiophysics, CSIRO, PO Box 76, Epping NSW 2121, Australia*

Received 1980 January 15; in original form 1979 October 31

Summary. Roberts 22 is a bipolar reflection nebula illuminated by a hidden A2 Ie star. Most of its energy is radiated at infrared wavelengths. It also shows strong OH maser emission (OH 284.18 – 0.79) on the 1612 and 1665 MHz transitions, generally similar to the masers associated with M stars having infrared excesses. But the system contains no late-type star.

This remarkable assemblage of attributes makes Roberts 22 unique; however, it is probably a key member of the newly-recognized population of bipolar nebulae.

From our analysis of the properties of Roberts 22 we question some published interpretations of other bipolar nebulae, in particular the derivation of spectral types for their underlying stars by the assumption of photoionization of the gas, and their evolutionary description as proto-planetary nebulae.

1 Introduction

1.1 OH 284.18 – 0.79

The source OH 284.18 – 0.79 is an OH maser showing intense emission, on both the 1612 and 1665 MHz transitions, over a wide velocity range (– 30 to + 20 km s^{-1}, LSR). At the time of its discovery (Manchester, Goss & Robinson 1969, where it was designated G 284.2–0.8), it appeared unique; in the light of subsequent OH surveys it is seen to resemble superficially the masers commonly associated with late-type (M) supergiants – a subclass of the type II OH/IR stars (Caswell 1974).

New observations, described in Section 2.2, have refined the position; the mean of three independent estimates measured at both 1612 and 1665 MHz is: $10^h\,19^m\,45^s.1 \pm 1^s.2$;

$-57°\,50'\,28'' \pm 10''$ (1950). An unresolved (< 4 arcsec) infrared source was located by Frogel & Persson (1975) at: $10^h\,19^m\,44^s.6$; $-57°\,50'\,41''$ (1950) and identified by them as the infrared counterpart of OH 284.18 – 0.79. This source, apart from its strong radiation in the 10–20 μm spectral region, bears little similarity to type II OH/IR stars, and was thought by Frogel & Persson to be a compact H II region because of the following properties:

(i) The 1.5–4 μm colours are better represented by an early-type star experiencing about 10 mag visual extinction than by a reddened or unreddened late-type star.

(ii) Frogel & Persson's data suggested the presence of a deep 3.1 μm ice absorption band, also indicative of high reddening and common in compact H II regions.

(iii) The colour temperature of the long-wavelength emission is unusually low for that associated with any types of galactic star, but resembles the values found in H II regions.

(iv) A faint, nebulous knot lies within a few arcsec of the infrared source.

No other infrared source near the OH error box was found by Frogel & Persson (1975). Deeper infrared searches were made using the Mount Stromlo Observatory infrared photometer on the 3.9-m Anglo-Australian telescope (AAT), and confirm that no other source is present to a limiting magnitude of +10 (60 mJy) at 2.2 μm. The identity of the OH and infrared sources seems certain.

1.2 ROBERTS 22

At the position of the infrared source found by Frogel & Persson (1975) is an emission-line object which has enjoyed a chequered history in the literature. It was discovered two decades ago by Henize (1976: Hen 404), who noted broad Hα emission and suspected it of being a Wolf–Rayet star. It therefore first appeared in print as entry 22 in Roberts' (1962) catalogue of Wolf–Rayet stars. Smith (1968) failed to record Roberts 22 on a blue objective-prism plate and therefore omitted it from her catalogue of Wolf–Rayet stars. Thus Wackerling (1970) listed it as a Be star. Sanduleak & Stephenson (1973) detected Hα and Hβ emission from Roberts 22 (therein listed as Wray 549) and suspected He II λ4686 emission; this qualified it for classification by them as a possible symbiotic star.

2 New observations of Roberts 22 = OH 284.18–0.79

None of the above classifications of the OH, infrared or visible objects appears to be correct.

In addition to the OH and infrared observations noted in Section 1.1, we have monitored the OH emission over several years using the Parkes 64-m radio telescope and have secured infrared photometry and optical spectra of Roberts 22. The latter were made using (i) the 74-inch Mt Stromlo telescope and Cassegrain image-tube spectrograph at 100 Å mm^{-1}; (ii) an image-dissector scanner (Robinson & Wampler 1972) on the AAT operating at resolutions of about 3 and 6 Å; and (iii) an image-photon counting system (Boksenberg & Burgess 1973) giving resolutions from 0.3 to 4.5 Å, also on the AAT. In addition we have been able to study the morphology of Roberts 22 on the integrating television camera of the AAT Cassegrain acquisition and guiding unit.

2.1 OPTICAL MORPHOLOGY

When studied in sub-arcsec seeing, Roberts 22 appears as a pair of irregular nebulae, A and B, separated in P.A. 30° by about 3.5 arcsec, and each of diameter about 2.5 arcsec. The magnitude difference between the components is between half and one magnitude. No

associated stellar object is seen to a limit of about 16th magnitude in the red. The appearance is that of a bipolar nebula, in which the two components are illuminated by a hidden star. Proof that this is the case will be given in Section 2.4.

2.2 OH OBSERVATIONS

Recent spectra of OH emission on the 1612, 1665 and 1667 MHz transitions are shown in Fig. 1. At 1612 and 1665 MHz the velocity structure has remained similar to that of the 1968 discovery observations (Manchester, Robinson & Goss 1970). With our improved sensitivity, emission at 1667 MHz is now apparent. The remaining ground-state transition near 1720 MHz shows no features, and at 1665 MHz spectra with wide velocity coverage ($\pm 900\,\mathrm{km\,s^{-1}}$) show no features other than those of Fig. 1. The mean LSR velocity of the two peaks is $-6 \pm 3\,\mathrm{km\,s^{-1}}$.

All transitions show relatively little net polarization: circular polarization measurements are shown in Fig. 1, and linear polarization measurements were given by Manchester *et al.* (1970).

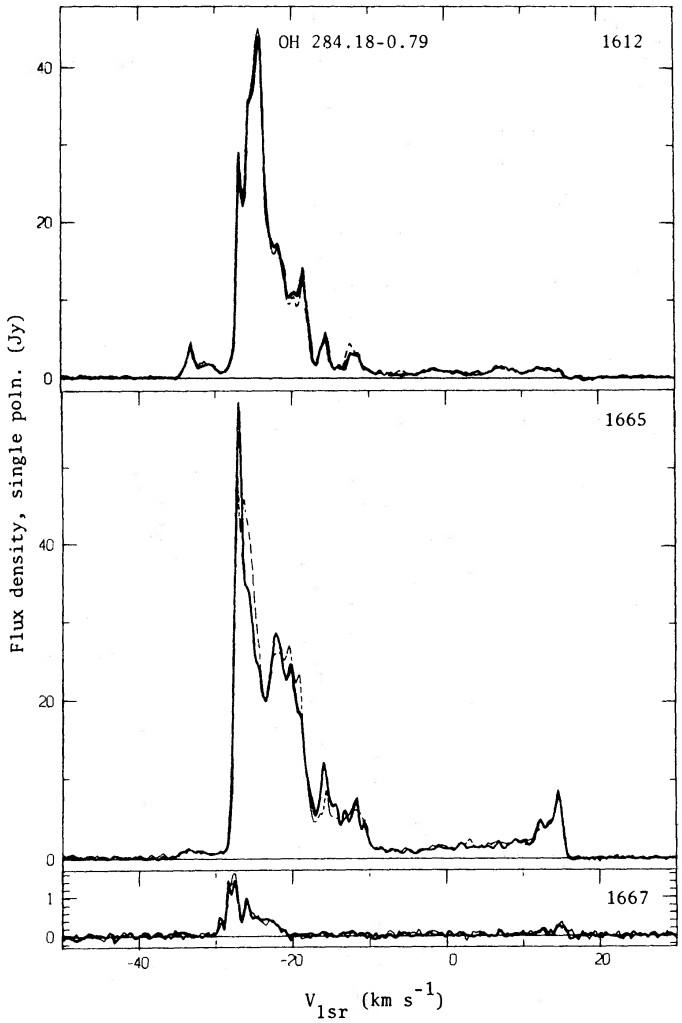

Figure 1. Representative ground-state OH spectra of OH 248.18−0.79 (= Roberts 22). Solid lines: right-hand circularly polarized component; broken lines; left-hand component. Taken 1978 August 18. Resolution $0.35\,\mathrm{km\,s^{-1}}$ (1.95 kHz).

Table 1. Variations in the OH intensity of OH 284.18–0.79.

Date	Integrated intensity of emission profile (10^{-22} W m^{-2})		
	1612 MHz	1665 MHz	1667 MHz
1968 (December?)	305	485	
1975 August	260	360	
1976 March	165	325	6.2
1976 July	165	280	6.0
1977 March	170	405	6.4
1977 September	250	415	5.6
1978 August	295	415	6.4

We have monitored the spectra of OH 284.18–0.79 at irregular intervals since its discovery. For all measurements the beam size was about 12 arcmin, and apart from the discovery observations, a dual-channel receiver was used followed by the Parkes autocorrelator (see e.g. Caswell & Haynes 1975). The same features are recognizable throughout the nine years. In Table 1 we summarize changes with time of the overall intensity; a periodicity of about three years may be present (as is most clearly suggested by the 1612 MHz data). However, a detailed comparison reveals a more complex picture:

(a) *1612 MHz variability.* Through the period 1968 to 1978 August essentially no changes have been detected in (i) the weak emission from -6 to $+15$ km s^{-1}, (ii) the emission near -33 km s^{-1}, which is outside the main range of velocities, and (iii) probably the feature at -16 km s^{-1}. By contrast, all the strong features between -6 and -28 km s^{-1} showed a drop to roughly half-intensity in the period 1976 March to 1977 March, and then recovered to their earlier values by 1978 August. The integrated flux density is dominated by these intense features.

(b) *1665 MHz variability.* At the two extreme epochs there are no marked differences, the circular polarization also remaining the same. At intermediate epochs the strong features between -6 and -28 km s^{-1} showed a significant drop in intensity (to about 60 per cent) in the period 1976 March–July; simultaneously the features between -7 and $+15$ km s^{-1} increased by a factor of about 2. A feature near -16 km s^{-1} and the (quite weak) emission at -33 km s^{-1} showed no perceptible change.

(c) *1667 MHz variability.* Despite our poorer sensitivity to this weak emission, it none the less seems that any variability is considerably less than on the other two transitions.

2.3 INFRARED OBSERVATIONS

We find the infrared source to lie within about 1 arcsec of the mid-point of the two nebulae. Our photometry at *J, H, K* and *L* appears to agree with that of Frogel & Persson (1975), although the latter is given only graphically. Our magnitudes at these wavelengths are, respectively, 8.64, 7.64, 7.00 and 5.08; errors on these are not more than ± 0.05 mag. The nature of the infrared continuum at all wavelengths greater than 2.2 μm is more typical of the dust continua found in regions surrounding hot, luminous stars than those associated with late-type stars.

We have additionally employed narrow-band filters centred at 2.1, 2.2 and 2.3 μm to search for the molecular features normally present in cool stars, and characteristic of M type OH/IR sources (Hyland *et al.* 1972). There is no evidence for H_2O absorption at 2.1 μm, nor of CO at 2.3 μm. Instead, the narrow-band colours can best be explained by a hot stellar

continuum reddened by 8–10 mag. A hot star reddened by about 10 mag is also consistent with the *J, H, K* magnitudes. The reddening estimate should be reduced if thermal emission from circumstellar dust contributes to the 2 μm flux, but the energy distribution suggests that such a contribution is negligible.

In an attempt to confirm the ice absorption at 3.1 μm reported by Frogel & Persson (1975), we secured a spectrum in the region 2.9–4.0 μm, using a circular variable filter with resolution $\lambda/\Delta\lambda \sim 50$. The spectrum shows at best a marginal ice absorption, and we estimate the optical depth in the ice band to be less than 0.3. An explanation of the apparently strong ice band found from filter photometry by Frogel & Persson may lie in the fact that the stellar and dust continua have roughly equal intensities at 3.1 μm, causing a broad minimum in the energy distribution. The 3.28 μm unidentified emission band (Russell, Soifer & Merrill 1977) appears moderately strongly in our spectrum of Roberts 22.

2.4 OPTICAL SPECTRA

Our observations of the two nebulae show them to have *identical* spectra. This is illustrated in Fig. 2, where raw spectra of A and B are presented together with their quotient. Broad features to the red of Hα in this quotient are caused by inaccuracies of the correction for field curvature near that end of the spectra. Note in particular the perfect cancellation of the very strong Hα and Hβ emission. This offers conclusive evidence that the two nebulae are illuminated by a common emission-line star.

The spectrum exhibits time-varying Balmer emission overlying Balmer absorption. Hβ ranges from strong emission (as in Fig. 2) to weak absorption, and the higher Balmer lines are more often present in absorption than in emission. The typical time scale of emission-line variation is one month or less. Numerous Fe II absorption lines are also seen; these are not visible on Fig. 2, which is at low signal-to-noise. On a red spectrogram taken at a time

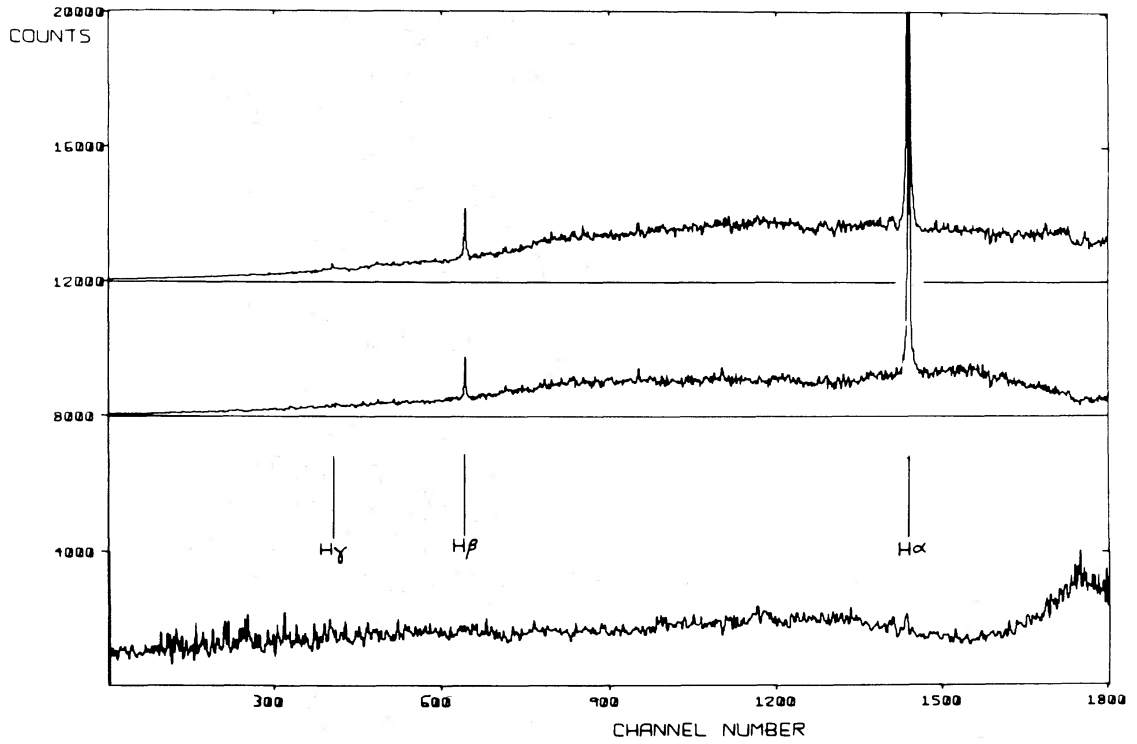

Figure 2. Raw low-dispersion spectra of Roberts 22. From top to bottom: component A; component B; ratio A/B.

when Hα was abnormally strong, Fe II was recorded in emission. The presence of Fe II absorption, and the absence of He I and the weakness of the Balmer absorption lines even at minimum Hα intensity indicate a spectral type near A2 Ie.

The Hα profile is shown in Fig. 3; its centroid lies at $+20 \pm 10\,\mathrm{km\,s^{-1}}$ LSR. The profile has wings extended to at least ±10 Å ($\pm 450\,\mathrm{km\,s^{-1}}$); on a lower dispersion scan of higher signal-to-noise the wings can be traced to double this velocity. The profile shows a broad absorption feature centred about $80\,\mathrm{km\,s^{-1}}$ to the blue of the emission peak. This is clearly of the P Cygni type, being far too strong to be produced by the underlying stellar absorption. The excellent cancellation shown in Fig. 2 places an upper limit of about $20\,\mathrm{km\,s^{-1}}$ on the velocity difference of the Hα emission reflected off the two wings.

Diffuse interstellar absorption lines are quite strong in the spectrum, although not seen in Fig. 2. Ca II *H* and *K*, and Na I *D* lines are also observed in absorption and are attributed to the same absorbing material. From the observed equivalent widths of the λλ6269–6284 blend (2.9 Å), and using Herbig's (1975a) data to relate line intensity to reddening, we derive $E_{B-V} \sim 3$–4 and hence $A_V \sim 10$ mag. Rather smaller values are found from the other interstellar lines, which are however less accurately measured.

We can make further estimates of A_V from our data. The ratio Hα/Hβ, after correction for the underlying stellar absorption, is about 15, corresponding to $A_V \sim 5$ if a case B Balmer decrement pertains. The continuum $B-V$ and $V-R$ colours of the nebulae also suggest $A_V \sim 5$. However, the reflected spectrum will be bluer than the emitted spectrum by an amount dependent upon the scattering law: the value of A_V for the reflected path to the star should be increased to ~ 9.5 mag for a λ^{-4} (Rayleigh) scattering law.

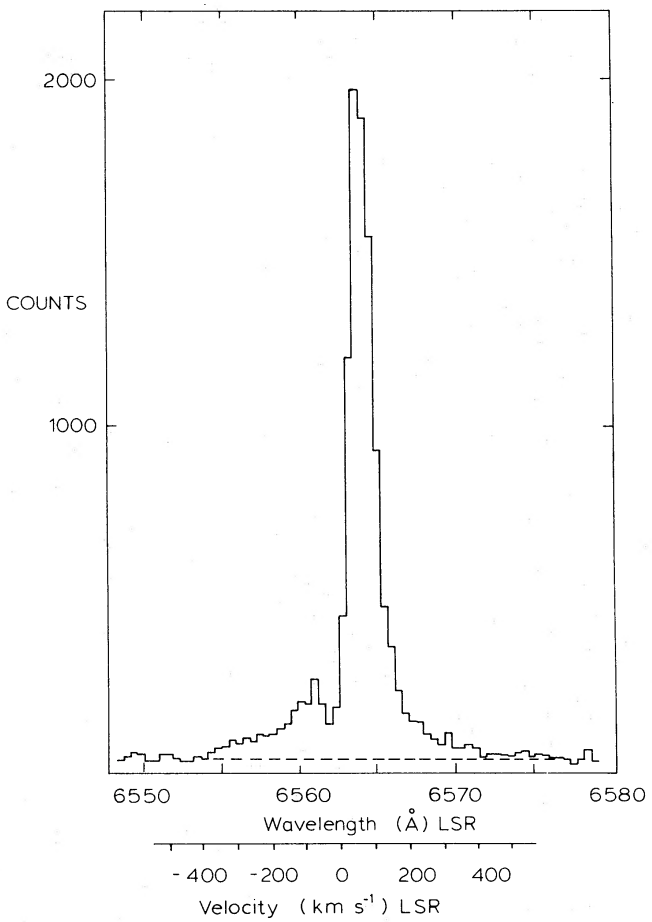

Figure 3. Profile of the Hα emission in Roberts 22A, showing the P Cygni absorption to the blue of the peak. Taken 1977 November 1. Resolution $14\,\mathrm{km\,s^{-1}}$ (0.3 Å).

3 The nature of Roberts 22

3.1 STRUCTURE

3.1.1 Geometric model

As already noted, the identity of the spectra from the two portions of the nebula indicates a common origin for both the continuous and the line emission components. We attribute this to reflection of the spectrum of an A2 Ie star lying between them. Extinction by circumstellar material naturally accounts for the absence of this star in the visible. We envisage a geometry similar to that of M1–92 (Herbig 1975b), namely a star lying within a compact nebula which is opaque near a plane (which we shall call the equatorial plane) and which scatters light from the polar clouds. We view the system at an angle θ to the equatorial plane.

The extinction must be higher along the direct line of sight to the star than along the reflected light path, otherwise the star would appear brighter than the nebulae. We derived similar values of A_V for the direct path (Section 2.3) and the reflected path (Section 2.4) to the star. This inconsistency is alleviated by a more critical analysis of both light paths.

For the *direct* light path through the equatorial ring a conventional reddening law does not appear to be applicable: the infrared colours lead to an R magnitude for the star $\sim 13.8 \pm 0.5$. No star is seen directly to a limit of $R \sim 16$. Thus $E_{R-K}/E_{J-K} \gtrsim 5.5$, compared to a more usual value 4.1. By extrapolation we infer that A_V on the direct light path considerably exceeds the 10 mag determined from the infrared colours.

For the *indirect* light path, the blueing effect was probably overestimated by the assumption of pure Rayleigh scattering. In the case of the similar object IV Zw 67 (CRL 2688), a scattering law proportional to λ^{-3} was found by Schmidt, Angel & Beaver (1978) and by Jones & Dyck (1978). If we use the same law for Roberts 22 we derive an A_V for the reflected light path of about 8 mag. It might also be argued that the lobes of the reflection nebula contribute significantly to the measured *J, H, K* fluxes (as found for IV Zw 67 by Ney *et al.* 1975). However, given the observed R magnitude of the nebula, no sensible scattering law will produce adequate infrared fluxes.

If we assume the reddening law on the reflected light path to be normal, we can remove its effect to derive an intrinsic R magnitude for the reflection nebulae of about 7.6. The dereddened K magnitude of the illuminating star is about 6.2 and for an A2 star $R-K$ is near zero. Hence the reflection nebulae must be almost optically thick to scattering, assuming that they subtend no more than 30 per cent of the sky to the star. Schmidt *et al.* (1978) found the NW lobe of M1–92 to be optically thick to scattering, and Cohen & Kuhi (1977) reached the same conclusion from the absence of limb-darkening in its lobes. The appearance of Roberts 22 at the telescope suggests that it exhibits little limb-darkening, but the object is too small for this to be anything but a marginal claim.

3.1.2 Velocities

Mass loss from the star, feeding the nebula, is indicated by the P Cygni Hα profile. The derived mass-loss velocity of about 80 km s^{-1} is lower than that of M1–92 by a factor of 7. As noted above, the cancellation of the spectra of the two wings limits their radial velocity difference to $\lesssim 20$ km s^{-1}. For an expansion velocity in the wings of v, the difference in measured velocity of the reflected spectra from the two is $2v \sin\theta$, and the mean stellar velocity is too positive by v. If we equate v to the P Cygni velocity of 80 km s^{-1}, the limit on velocity difference would imply that we are viewing Roberts 22 from within about 7° of the equatorial plane. However, from the appearance and relative brightness of the two

components, we suggest that $\theta \sim 20$–$30°$. For $\theta = 30°$, $v \lesssim 20\,\mathrm{km\,s^{-1}}$. A correction no greater than $20\,\mathrm{km\,s^{-1}}$ should therefore be subtracted from the mean Hα velocity, and this brings it into close agreement with the OH data. This line of reasoning parallels that used by Herbig (1975b) in the case of M1–92.

The emission zone has a typical velocity range, determined as the standard deviation of the Hα emission profile, of $170\,\mathrm{km\,s^{-1}}$. Between the emission zone and the polar nebulae is a decelerating region of neutral hydrogen, which provides the Hα absorption component and has an effective expansion velocity of $80\,\mathrm{km\,s^{-1}}$. We locate the OH emission zone in the outer parts of the nebula, where the gas is decelerating only slightly. Only here can be found significant path lengths with velocity dispersion sufficiently small to permit OH maser emission. The separation of the main OH peaks is consistent with our limit on the velocity of the polar nebulae.

3.1.3 The equatorial ring

The most opaque, and therefore densest portion of the nebula lies in the equatorial plane, presumably taking the form of a ring of material encircling the star. Here we locate most of the radiation beyond 3 μm. The infrared energy distribution measured by Frogel & Persson (1975) is broader than that of a blackbody, but a colour temperature near 200 K is appropriate to the dust which provides most of the flux. Since the optical thickness to the centre of the nebula exceeds 7 at V, that at 10 μm is probably greater than 0.3. If the dust formed a sphere of this optical thickness, the angular diameter would be nearly 2 arcsec. The fact that the dust is much less thick over the poles has small effect on this figure, whereas an error of 50 K in the colour temperature changes the diameter by a factor of 2. The emitting dust therefore lies mostly within the dark lane.

3.2 DISTANCE-DEPENDENT PARAMETERS

3.2.1 Distance

We have no reliable estimate of the distance to Roberts 22. We may derive a naïve estimate by combining the dereddened 2.2 μm magnitude of the object, 6.2 mag, with a spectral type of A2 Ib. This yields a distance of 1.8 kpc. A distance of about 2.4 kpc is indicated by the mean OH radial velocity of $-6\,\mathrm{km\,s^{-1}}$ using standard galactic rotation models. But a modest peculiar motion (of up to $6\,\mathrm{km\,s^{-1}}$) would allow any distance between 0 and 5 kpc. We adopt a value of 2 kpc.

3.2.2 Luminosity

The luminosity of Roberts 22 is very poorly determined, in part because of the uncertain distance and in part because observations have not been made to sufficiently long wavelength. A blackbody extrapolation of the infrared component (which carries most of the energy) suggests that the radiated energy is not very different from that expected of an A2 supergiant. Specifically, for a distance of 2 kpc, we find $2 \times 10^4\ L_\odot$.

3.2.3 Nebular mass

We can estimate the mass of dust in the nebula from the formula:

$$M_\mathrm{d} = \frac{4}{3}\pi a^3 \rho \frac{\Omega D^2}{\pi a^2 Q_\lambda} \phi\tau$$

where the first term gives the mass of a grain of radius a and density ρ, and the remaining terms give the number of grains in a nebula subtending a solid angle Ω at a distance D. Here Q_λ is the grain absorption efficiency, τ is the nebula's optical depth at wavelength λ, and ϕ is a geometrical factor which ranges from $\frac{1}{3}$ (for a solid sphere of dust) to unity (for an infinitely thin shell). For Roberts 22 we adopt $\phi = \frac{2}{3}$, since the infrared emission is so broad as to indicate a range of temperatures. We also use $\tau = 1$ at a wavelength of $5\,\mu$m (Section 3.1.3), and $\rho = 2$. For the canonical dust to gas ratio of 100, the mass of the equatorial ring is $250 a/Q_5\, M_\odot$ where a/Q_5 is in cm. The choice of a value of a/Q_5 is now arbitrary, according to the composition, size, shape and purity of the grains in the nebula. A credible range of this parameter is from λ to unity, and this corresponds to a nebular mass between 0.1 and $250 M_\odot$. The preferred value of this parameter is $\sim 10^{-3}$ (see Gilman 1974, for data on olivine, iron, silicon carbide and graphite), giving a mass $\sim 0.3 M_\odot$. The mass refers primarily to the equatorial ring.

3.3 THE EMISSION LINES

A2 supergiants cannot provide sufficient Lyman continuum photons to account for the Balmer emission seen in Roberts 22. From the observed mean equivalent width of Hα, 50 Å, we have estimated the dereddened line intensity, and hence have derived a value of $N_e{}^2 V \sim 4 \times 10^{59}$ cm^{-3}. This implies a luminosity of $500 L_\odot$ in the Lyman continuum, which corresponds to an O9.5 ZAMS star (Panagia 1973).

The luminosity of Roberts 22 is not inconsistent with that of an O star. Such a star could lie within an optically thick shell or wind which masquerades as an A2 supergiant. Any geometry which permitted the O star's Lyman continuum to escape and ionize the gas would, however, seem rather contrived.

A natural source of ionization is provided by deceleration of the outflowing gas. It is unlikely, however, that collisional ionization occurs in the polar directions, where there seems to be a steady deceleration from > 80 to 20 km s^{-1} through the polar nebula. Rather, we believe that the outflowing gas encounters a dense equatorial ring which has little or no radial velocity. In this mode, the H I emission arises at the shock interface of the stellar wind and the ring. Fig. 4 is a sketch of the geometry we envisage for Roberts 22.

We use 170 km s^{-1} as the gas velocity, being the width of the Hα profile. This might be an underestimate. If the gas is halted and its kinetic energy used in ionization, we require that $2 \times 10^{-4} M_\odot$ yr^{-1} be striking the disc. The total mass loss from the star would be higher by a geometrical factor perhaps as large as 3. The required mass loss is embarrassingly high. For comparison, the A supergiant α Cygni loses $10^{-8} M_\odot$ yr^{-1} (Lamers, Stalio & Kondo 1978), and the extreme star P Cygni attains only $2 \times 10^{-5} M_\odot$ yr^{-1} (Barlow & Cohen 1977; van Blerkom 1978).

We may place an upper limit of a few hundred years on the time-scale over which such mass loss has occurred, however, from the physical dimensions in the polar directions and for polar velocities of 20 km s^{-1}. In that time, less than one solar mass would be lost. An A supergiant or late O star would have a mass of about $20 M_\odot$. A brief period of such extreme mass loss cannot be ruled out, therefore. If, indeed, evolution of the nebula proceeds on so rapid a time-scale, we might hope to see changes in a few decades.

We are unable to estimate the mass-loss rate from the P Cygni absorption since we have no handle on the teperature of the neutral gas, a parameter which critically determines the population in the lower level of the Hα transition.

The interaction of a disc or ring and a stellar wind has been discussed by Elmegreen (1978). Viscosity in the ring causes it to infall while the stellar wind removes material

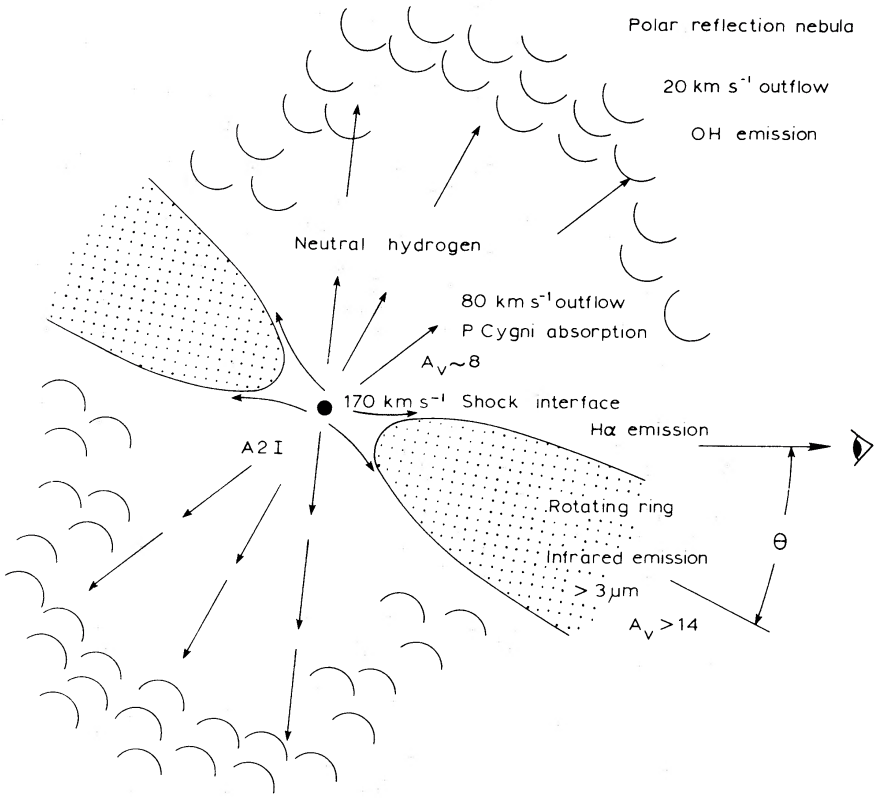

Figure 4. Schematic cross-section of Roberts 22.

from the shocked interface. Lyndon Bell & Pringle (1974) estimate the infall velocity to be 10^{-3} of the orbital velocity. In the case of Roberts 22, the infall velocity can be at most a few metres per second. For this reason we do not locate the OH emission within the ring.

3.4 OH EMISSION

We first note the general similarity of the 1612 MHz emission to that of the late-type stars, and in particular to the supergiants VY CMa and NML Cyg (Caswell 1974). As in these stars, the high brightness temperatures and non-LTE intensity ratios argue that the emission is generated by a maser process, and in the case of the 1612 MHz transition, pumping by far-infrared radiation (35 μm?) is quite likely responsible (Elitzur, Goldreich & Scoville 1976). The existence of strong infrared emission from Roberts 22 thus strengthens its identification with the OH source, which is good on positional grounds alone.

The presence of OH emission indicates that the source should possess an oxygen-rich envelope. Although the expected 10 μm silicate emission feature is absent, Persson, Frogel & Aaronson (1976) attribute this to the presence of overlying silicate absorption.

We now consider four properties of the OH emission which need to be accommodated in any detailed model of the source.

3.4.1 OH velocity structure

The velocity structure of all three transitions shows the two peaks characteristic of OH/IR late-type stars. Caswell's (1974) interpretation that the peaks arise from the front and rear of an expanding shell is now generally accepted for the late-type stars. The quite smoothly defined intensity–velocity envelopes at both 1612 and 1665 MHz argue that the OH

intensity is only a linear function of maser path length, as is expected for saturated (pump-limited) masers (see also Section 3.4.2). The 1612 and 1665 MHz emission at $-26\,\mathrm{km\,s^{-1}}$ from the mean reveals material moving at velocities higher than the general expansion (or infall) velocity of $20\,\mathrm{km\,s^{-1}}$. Similar 'high-velocity' features are seen in several of the most intense OH/IR late-type stars. Interferometry is desirable to check further on the geometry. By analogy with other stars, the total size may be several arcsec.

3.4.2 Polarization

The low polarization at 1612 MHz is common in the late-type stars; the low polarization at 1665 MHz is unusual, but we suggest it results from the blending of many quite narrow features. If the occasional intense, narrow features are typical of those which make up the composite profile, considerable overlapping of features must be occurring.

3.4.2 Time variability

The observed time variability suggests that a check should be made for a correlation with any infrared variability; for most late-type stars the correlation is good, suggesting that the maser emission is saturated ('pump-limited').

3.4.4 Relative line strengths

An unusual characteristic of the OH emission is the relative line strengths: the 1665 MHz emission is comparable in intensity with the 1612 MHz emission, and (from the velocity comparison) seems to be coextensive with it. The 1667 MHz emission is much weaker but also roughly coextensive.

Most of the above properties are shared by the M-type OH/IR stars except for the last one. Elitzur *et al.* (1976) confined their attention to 1612 MHz emission, for which 35 μm photons from dust provide a satisfactory pump. Since the dust cloud is paramount, their scheme (devised for M-type giants and supergiants) seems adequate in the case of Roberts 22. More recently Elitzur (1978) has proposed a scheme to account for *main-line* OH emission from such circumstellar shells; it relies on deviations from a blackbody in the spectrum of optically thin dust due to the grain properties. In general, higher dust temperatures favour the 1665 MHz transition and lower OH densities tend to favour main-line rather than 1612 MHz emission. It is not clear whether Elitzur's scheme as it stands could account for the quite high intensity of 1665 MHz emission that is found in Roberts 22; however, if, as in Elitzur's model, the dust temperature and grain properties are crucial, then the early spectral type of Roberts 22 may be responsible for dust properties which are systematically different from those of the late M-type stars, and thus indirectly promote 1665 MHz maser emission.

An alternative model of collisional pumping as suggested by Elitzur & de Jong (1978) for main-line masers near compact H II regions seems less acceptable in the environment of Roberts 22; however, our requirement of a strongly shocked region to account for Hα emission (Section 3.3) might be relevant to this possibility.

We finally note that no H_2O maser has been detected in Roberts 22 as yet; this is fairly unusual for a strong main-line OH maser of either the compact H II region or the late-type star varieties.

3.5 EVOLUTIONARY STATUS

Roberts 22 must be either pre- or post-main-sequence. Mass loss can occur at either according to current thinking. We cannot easily distinguish the two possibilities but we favour a

pre-main-sequence age because we can envisage no plausible mechanism whereby mass loss alone could produce or sustain a shocked ring like that apparently surrounding Roberts 22. Unfortunately, our estimate of the nebular mass (Section 3.2.3) does not preclude an origin in post-main-sequence mass loss. Any data which might narrow the range of the parameter a/Q_S would be valuable in this regard.

Equatorial rings are commonly found in association with the collapsing phase of stellar formation. A classic example of this is Lk Hα 208 (pictured in Herbig 1960), also involved in a bipolar nebula. The ring around Roberts 22 must be at an early stage of its collapse, for it retains appreciable thickness in the polar direction. We would expect such a ring to be dispersed during the main-sequence lifetime of Roberts 22, or else to form planets.

A weak argument favouring relative youth is the proximity of Roberts 22 to the H II regions RCW 48 and 49. The proximity extends to the third dimension if our estimated distance is reasonable, but since at this galactic longitude we look directly along a spiral arm, the probability of a chance alignment must be rather high.

4 Is Roberts 22 unique?

No other object is known which combines the morphology, OH, infrared and spectral properties of Roberts 22. However, several objects have similar morphology and strong infrared emission. M1–92 and IV Zw 67 have already been alluded to; CRL 618 (Westbrook *et al.* 1975), V645 Cyg (Cohen 1977) and Hen 401 (Allen 1978), also come to mind. In each of these the illuminating star is, as in Roberts 22, totally obscured in the visible.

If the clearer polar cones typically subtend 90° at the star, in 30 per cent of cases we will view the star through that pole.* The nebula may then be difficult to detect, and such objects would be less easily recognized. One diagnostic might be strong infrared emission for unusually small reddening. A number of objects meet that criterion, but we note in particular IRC +10 420 (Humphreys *et al.* 1973), which has an F supergiant spectrum and is outsanding for the discovery, by Giguere, Woolf & Webber (1976), of strong 1612 and 1667 MHz OH emission. The object is known to be extended (Thompson & Boroson 1977) but is probably dominated by the central star at optical wavelengths. In any case it is too small to be seen in any detail. Mutel *et al.* (1979) mapped the distribution of OH masers in IRC +10 420 and deduced the presence of a disc in that system.

To aid in comparing these objects we have drawn together in Table 2 their relevant properties. Except where indicated, these have been abstracted from the references cited above. At first sight the objects appear unrelated. But Roberts 22 acts as a missing link, for (with the possible exception of polarization, which we have not measured) it combines all their properties.

Among the objects listed in Table 2, the presence or absence of any OH maser may be chiefly dictated by the C/O ratio; indeed two of the sources that fail to show OH emission appear carbon-rich. Three objects show detectable OH emission: as we pass through the sequence of spectral types F through A to B, main-line emission (either 1665 or 1667 MHz) changes from being weaker than 1612 MHz to equality, and finally dominates. This may be significant in connection with the main-line pump mechanism discussed in Section 3.4.4. We recall that renewed interest in Roberts 22 was stimulated by the OH properties (Frogel & Persson 1976; this paper); other strong 1612 MHz OH masers may be similar to the bipolar nebulae of Table 2, rather then being late-type (M) stars. A possible diagnostic is relatively intense main-line emission with velocity spread coextensive with (or wider than) the 1612 MHz emission.

* This assumes that the orientation of the nebulae is random. The assumption seems justified, since the known examples show no preference for alignment in galactic coordinates.

Table 2. Properties of some objects which resemble Roberts 22.

	Roberts 22	V645 Cyg	CRL 618	M1-92	Hen 401	IV Zw 67	IRC +10 420
V of nebula (mag)	13:	14.7	17.0	11.7	14:	12.3	11.2
A_V to star (mag)	>10	-	Large	10?	-	Large	6.5
Appearance	Bipolar	Bipolar	Bipolar	Bipolar	Bipolar	Bipolar	Stellar
Separation of nebulae (")	3.5	7	7	8	6	8	
Magnitude difference	~1	0.6	1.3	2	Small	2	
Spectral type	A2 Ie	O7 Ve*	O9-B1 e*	B0.5 (V)e	B e*	F5 Iae†	F8 Ia-Iab
Emission lines	HI, FeII	HI, HeI, FeII, [] lines	HI, HeI, [] lines	HI, HeI, FeII, [] lines	HI, HeI, FeII, [] lines	Hα filled in, C_2, [SII]	
P Cyg velocity (km s^{-1})	80	650		530			
Linear polarization (%)	-	14	21	25	-	50	
10 μm flux (Jy)	60	60	350	14	-	270	2000
Dust colour temperature (K)	200	450	280	~1000	-	150	270
Galactic longitude	284°.2	94°.6	166°.5	64°.1	285°.1	80°.2	47°.1
" latitude	-0°.8	+1°.8	-6°.5	+4°.3	-2°.7	-6°.5	-2°.5
Distance (kpc)	2:	6	-	<4.5	-	1	4-7
z (pc)	30:	190	-	<330	-	110	180-300
OH properties	Strong: 1612 ≈ 1665 ⩾ 1667	-	§	Very weak: 1667 > 1612‡	No emission at 1665 or 1667 MHz	§	Strong: 1612 > 1667 ⩾ 1665
ΔV (km s^{-1})	50	-	-	Broad	-	-	58

*Spectral type derived by assuming photoionization of gas.
†Crampton, Cowley & Humphreys (1975).
‡Lépine & Rieu (1974); Fix & Mutel (1977).
§No OH emission; probably carbon-rich.

According to the literature, the central stars of the objects of Table 2 range widely in spectral type and luminosity class. In many cases the spectral type was determined on the assumption that the emission spectrum is excited by photo-ionization. We have shown that this is not necessarily the case in Roberts 22, and therefore question the validity of the assumption in other examples. It seems attractive to consider all the underlying stars to be pre-main-sequence, either O stars hidden in optically thick shells, or F, A or B supergiants. The intensity of the emission spectrum then derives from the mass-loss velocity rather than the spectral type of the underlying star.

Our argument that Roberts 22 is a pre-main-sequence object applies equally to other objects in Table 2. In this we are at odds with Westbrook *et al.* (1975), Zuckerman *et al.* (1976), Lo & Bechis (1976), and others who argue that IV Zw 67 and CRL 618 are proto-planetary nebulae. We consider that none of these authors has successfully explained the morphology of the objects, and that their assumption of photo-ionization is insecure. For IRC +10 420 Mutel *et al.* (1979) presented a consistent model involving a 30 $M_{\odot}$ star in the course of post-main-sequence evolution. Our model agrees with Cohen & Kuhi (1977), who interpret M1–92 (but not IV Zw 67) as a pre-main-sequence object.

The objects in Table 2 probably have disc geometries and are losing mass. The infrared emission, the one common property which is not aspect-dependent, might offer the most certain means of detecting more such objects. Recognizing those which are viewed from above the poles will still prove difficult. We suggest that Roberts 22 provides us with a yard-stick by which subsequent discoveries of similar objects may be classified.

Acknowledgments

We thank R. F. Haynes and W. M. Goss, who participated in the OH study.

References

Allen, D. A., 1978. *Mon. Not. R. astr. Soc.*, **184**, 601.
Barlow, M. J. & Cohen, M., 1977. *Astrophys. J.*, **213**, 737.
Boksenberg, A. & Burgess, D. E., 1973. *Proc. Symp. Astronomical Observations with Television-Type Sensors*, held at the Institute of Astronomy and Space Science, Vancouver, May 1973, p. 21, eds Glaspey, J. W. & Walker, G. A. H.
Caswell, J. L., 1974. *Proc. IAU Symp. No. 60, Galactic Radio Astronomy*, p. 423, eds Kerr, F. J. & Simonson, S. C., Reidel, Dordrecht.
Caswell, J. L. & Haynes, R. F., 1975. *Mon. Not. R. astr. Soc.*, **173**, 649.
Cohen, M. 1977. *Astrophys. J.*, **215**, 533.
Cohen, M. & Kuhi, L. V., 1977. *Astrophys. J.*, **213**, 79.
Crampton, D., Cowley, A. P. & Humphreys, R. M., 1975. *Astrophys. J.*, **198**, L135.
Elitzur, M., 1978. *Astr. Astrophys.*, **62**, 305.
Elitzur, M. & de Jong, T., 1978. *Astr. Astrophys.*, **67**, 323.
Elitzur, M., Goldreich, P. & Scoville, N. Z., 1976. *Astrophys. J.*, **205**, 304.
Elmegreen, B. G., 1978. *Moon Planets*, **19**, 268.
Fix, J. D. & Mutel, R., 1977. *Astrophys. Lett.*, **19**, 37.
Frogel, J. A. & Persson, S. E., 1975. *Astrophys. J.*, **197**, 351.
Giguere, P. T., Woolf, N. J. & Webber, J. C., 1976. *Astrophys. J.*, **207**, L195.
Gilman, R. C., 1974. *Astrophys. J. Suppl.*, 28, 397.
Henize, K. G., 1976. *Astrophys. J. Suppl.*, **30**, 491.
Herbig, G. H., 1960. *Astrophys. J. Suppl.*, **4**, 337.
Herbig, G. H., 1975a. *Astrophys. J.*, **196**, 129.
Herbig, G. H. 1975b. *Astrophys. J.*, **200**, 1.
Humphreys, R. M., Strecker, D. W., Murdock, T. L. & Low F. J., 1973. *Astrophys. J.*, **179**, L49.
Hyland, A. R., Becklin, E. E., Frogel, J. A. & Neugebauer, G., 1972. *Astr. Astrophys.*, **16**, 204.

Jones, T. J. & Dyck, H. M., 1978. *Astrophys. J.*, **220**, 159.
Lamers, H. G. J. L. M., Stalio, R. & Kondo, Y., 1978. *Astrophys. J.*, **223**, 207.
Lépine, J. R. D. & Nguyen-Quang-Rieu, 1974. *Astr. Astrophys.*, **36**, 469.
Lo, K. Y. & Bechis, K. P., 1976. *Astrophys. J.*, **205**, L21.
Lynden-Bell, D. & Pringle, J. E., 1974. *Mon. Not. R. astr. Soc.*, **168**, 603.
Manchester, R. N., Goss, W. M. & Robinson, B. J., 1969. *Astrophys. Lett.*, **3**, 11.
Manchester, R. N., Robinson, B. J., & Goss, W. M., 1970. *Aust. J. Phys.*, **23**, 751.
Mutel, R. L., Fix, D., Benson, J. M. & Webber, J. C., 1979. *Astrophys. J.*, **228**, 771.
Ney, E. P., Merrill, K. M., Becklin, E. E., Neugebauer, G. & Wynn-Williams, C. G., 1975. *Astrophys. J.*, **198**, L129.
Panagia, N., 1973. *Astr. J.*, **78**, 929.
Persson, S. E., Frogel, J. A. & Aaronson, M. 1976. *Astrophys. J.*, **208**, 753.
Roberts, M. S., 1962. *Astr. J.*, **67**, 79.
Robinson, L. B. & Wampler, E. J., 1972. *Publs astr. Soc. Pacif.*, **84**, 161.
Russell, R. W., Soifer, B. T. & Merrill, K. M., 1977. *Astrophys. J.*, **213**, 66.
Sanduleak, N. & Stephenson, C. B., 1973. *Astrophys. J.*, **185**, 899.
Schmidt, G. D., Angel, J. R. P. & Beaver, E. A., 1978. *Astrophys. J.*, **219**, 477.
Smith, L. F., 1968. *Mon. Not. R. astr. Soc.*, **138**, 109.
Thompson, R. I. & Boroson, T. A., 1972. *Astrophys. J.*, **216**, L75.
van Blerkom, D., 1978. *Astrophys. J.*, **221**, 186.
Wackerling, L. R., 1970. *Mem. R. astr. Soc.*, **73**, 153.
Westbrook, W. E., Becklin, E. E., Merrill, K. M., Neugebauer, G., Schmidt, M., Willner, S. P. & Wynn-Williams, C. G., 1975. *Astrophys. J.*, **202**, 407.
Zuckerman, B., Gilra, D. P., Turner, B. E., Morris, N. & Palmer, P., 1976. *Astrophys. J.*, **205**, L15.